Synsint Research Group

Available online at www.synsint.com

Synthesis and Sintering

ISSN 2564-0186 (Print), **ISSN** 2564-0194 (Online)

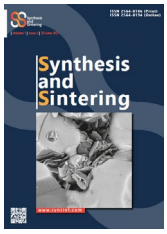

Research article

Corrosion and mechanical behavior evaluation of in-situ synthesized Cu-TiB_2 nanocomposite

Hossein Aghajani [a,*], **Seyed Ali Naziri Mehrabani** [b], **Arvin Taghizadeh Tabrizi** [a], **Falih Hussein Saddam** [c]

[a] *School of Metallurgy and Materials Engineering, Iran University of Science & Technology, Narmak, Tehran, Iran*
[b] *Nano Science and Nano Engineering Department, Istanbul Technical University, Maslak, Istanbul, Turkey*
[c] *College of Engineering, Thi-Qar University, Thi-Qar, Iraq*

A B S T R A C T

In this paper, the synthesis of the copper matrix nanocomposite and the effect of adding TiB_2 nanoparticles on the copper matrix have been investigated. Three different amounts of TiB_2 nanoparticles 5, 10, and 15 wt% were added and sintering was carried out at 900 °C for 4 hours under argon atmosphere. The phase formation of achieved nanocomposites was studied by X-ray diffractometer and the morphology of the synthesized samples was studied by field emission scanning electron microscopy and atomic force microscopy. The polarization and electrochemical impedance spectroscopy (EIS) applying 3.5 wt% NaCl solution at room temperature was carried out to evaluate the corrosion behavior of synthesized samples. Results show that adding the TiB_2 nanoparticles decreases the corrosion resistance by forming galvanic couples, but the effect the amounts of porosities have on the corrosion resistance is higher. It is revealed that the variation of the surface roughness is in direct relation to the value of polarization current density.

© 2021 The Authors. Published by Synsint Research Group.

KEYWORDS

Nanocomposite
Corrosion behavior
Cu-TiB_2
Surface roughness

OPEN ACCESS

1. Introduction

Applications of copper-based materials are commonplace due to their excellent properties such as electrical and thermal conductivity, easy fabrication, and being cost-effective, which make them suitable for a wide range of applications, for instance, spot welding electrodes. Some structural drawbacks such as low hardness, low tensile strength, and poor wear resistance are assigned as the limitations of copper-based materials. In addition, the mechanical strength of copper-based materials can be affected and lost in some harsh environments [1]. Age hardening and incorporation of a hard second phase are two common ways to add to these limitations. The first method, age hardening, is related to the addition of zirconium or chromium to copper and the precipitation of a hard second phase. Nevertheless, the lack of strength above 500 °C was observed due to the structural instability, which resulted from the coarsening of the precipitated phase [2, 3]. However, incorporation of the second phase to copper as the reinforcement led to increased temperature strength, hardness, and wear resistance. The reinforcement elements such as oxides, borides, and carbides are utilized to reduce the extent of wear deformation in the subsurface regions [4–6].

Copper-based metal matrix composites (Cu-MMCs) investigations have continuously been done to achieve enhanced physical and mechanical properties for industrial applications such as contact supports and fractional brake parts, electronic contact devices, high-temperature performance switches, and brake discs [7, 8]. Some different synthesis methods for instance infiltration [9], hot isostatic pressing (HIP) [10], powder metallurgy (PM) [2, 11], self-propagating

* Corresponding author. *E-mail address:* haghajani@iust.ac.ir (H. Aghajani)
Received 28 May 2021; Received in revised form 8 June 2021; Accepted 29 June 2021.
Peer review under responsibility of Synsint Research Group. This is an open access article under the CC BY license (https://creativecommons.org/licenses/by/4.0/).
https://doi.org/10.53063/synsint.2021.1228

high-temperature synthesis (SHS) [12], and spark plasma [13] as well as stir casting was reported for obtaining copper-based MMCs. In the stir casting method, reinforcements are added to the metal matrix in the molten state. Powder metallurgy, as a conventional method with a high production rate, is based on sintering the sample after metal powder pressing to demanded shape [13]. Good binding at the interface is mentioned as the conventional problem for ceramic reinforced metal matrix composites, which is associated with the low dissolvability of ceramics in most metals [14]. The in-situ synthesis method is preferred to the others due to the homogenous reinforcement, excellent surface bonding, and pure inter-phase [7].

Aside from the various synthesis methods, proper reinforcement plays a critical role in fabricating the composite with desired properties. The effect of different reinforcement elements such as Al_2O_3 [7], TiO_2, ZrO_2 [15], and TaC [16] on the MMCs, especially copper-based ones, have been studied widely. Investigating the additional amount of B_4C revealed improvements in both wear resistance and hardness [17]. On the other hand, Moustafa et al. [18] found that the Cu-MMC with graphite reinforcement possesses a lower frictional coefficient and wear rate instead of reducing hardness. On the other hand, some studies showed the significant enhancement of mechanical properties of copper composite by adding different carbon sources such as graphene, graphite and CNTs [19–23]. Meanwhile, higher modulus and stable thermodynamic properties of TiB_2 make it an appropriate reinforcement for high mechanical strength purposes. Therefore, in our previous work [24], which aimed at the formation of TiB_2, produced nanocomposite by SHS method in a ternary system of Cu-Ti-B was studied, but due to the thermodynamical and kinetic conditions, no TiB_2 phase was formed. So, to investigate the effect of TiB_2, in this paper, the in-situ method was carried out to fabricate the composites with various amounts of TiB_2 to investigate the effect of the reinforcement on corrosion resistance.

2. Experiments

2.1. Raw materials and synthesis method

Pure copper powders (99% purity, with a mean particle size of 50 µm, Merck) and TiB_2 powders (99% purity, with a mean particle size of 60 µm, Merck) have been used as raw materials. For the synthesis of nanocomposites, different weight percent of nanoparticles as reinforcements were prepared, which were 5, 10, and 15 wt% TiB_2, respectively, as is shown in Table 1. The powders were mixed mechanically by ball mill with an initial ball-to-powder weight ratio (BPR) = 10:1 at 300 rpm for 7 hours under argon atmosphere. Then, the cold press was carried out under 20 MPa pressure to obtain disc shape samples with a diameter of 20 mm and a height of 10 mm. Sintering was carried out at a tube furnace (Tube Furnace-Nardin) under an Ar atmosphere at 900 °C for 4 hours with a heating rate of 5 °C/min. In the end, all the specimens were cooled in the furnace down to the ambient temperature.

2.2. Characterizations

Vickers microhardness tests were carried out to evaluate the surface microhardness of achieved synthesized nanocomposites. Surface morphology of samples had been studied by using Field Emission-Scanning Electron Microscopy (FE-SEM-Vega Tescan) with EDS (Energy Disperse X-ray Spectroscopy) and also Atomic Force Microscopy (AFM), and microstructure, elemental, and topographical analysis, were carried out respectively. The corrosion resistance of the sample was analyzed by electrochemical polarization test (iVium), which was done in 150 ml 3.5% NaCl contained standard three-electrode configuration corrosion cell at the rate of 1 $mV.s^{-1}$ at room temperature. Meanwhile, Electrochemical Impedance Spectroscopy (EIS) was implemented at 10^{-5} to 90 kHz frequency range with 3 mV amplitude in a Solartron 1470 battery to evaluate the corrosion behavior of products.

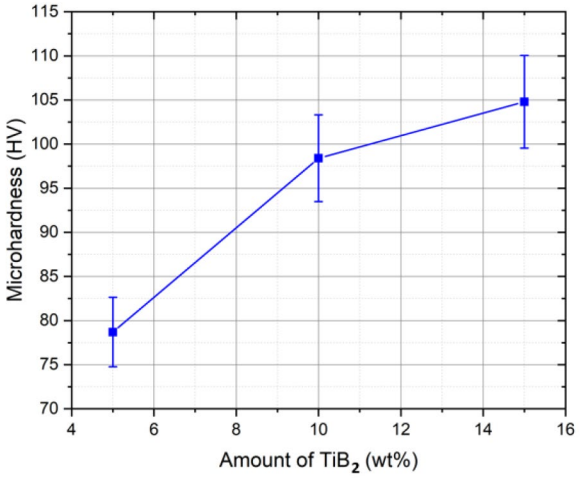

Fig. 1. Microhardness values of samples.

3. Results and discussion

Mechanical properties of samples were evaluated through the Vickers microhardness tests and the measured values are presented in Fig. 1. It was observed that as expected, adding the TiB_2 nanoparticles increase the microhardness. The surface microhardness of the copper sample, without any added reinforcement, equals 50 HV. Therefore, it is shown that the addition of reinforcements has an almost 100% efficiency in increasing the surface hardness, and the maximum value was obtained in the sample 85CT, with 15 wt% of TiB_2, which was 104.8 HV. Another reason for the remarkable increase is the proper dispersion of the TiB_2 nanoparticles in this sample. MAP analysis images, provided in Fig. 2, confirm this acclaim and dispersion of these reinforcements in the copper matrix and shows the homogenous and uniform distribution of TiB_2 nanoparticles. The marked areas by a circle in the images of Fig. 2, exhibit the presence of TiB_2 nanoparticles. It is worth mentioning that the maximum obtained surface hardness is much lower than the surface hardness of SHS-produced copper-based nanocomposite in our previous study [24], equaling 544 HV. The formation of multiple phases including TiO and Cu_3Ti had more effect

Table 1. The coding of samples.

Composition	TiB_2 content (wt%)
95CT	5
90CT	10
85CT	15

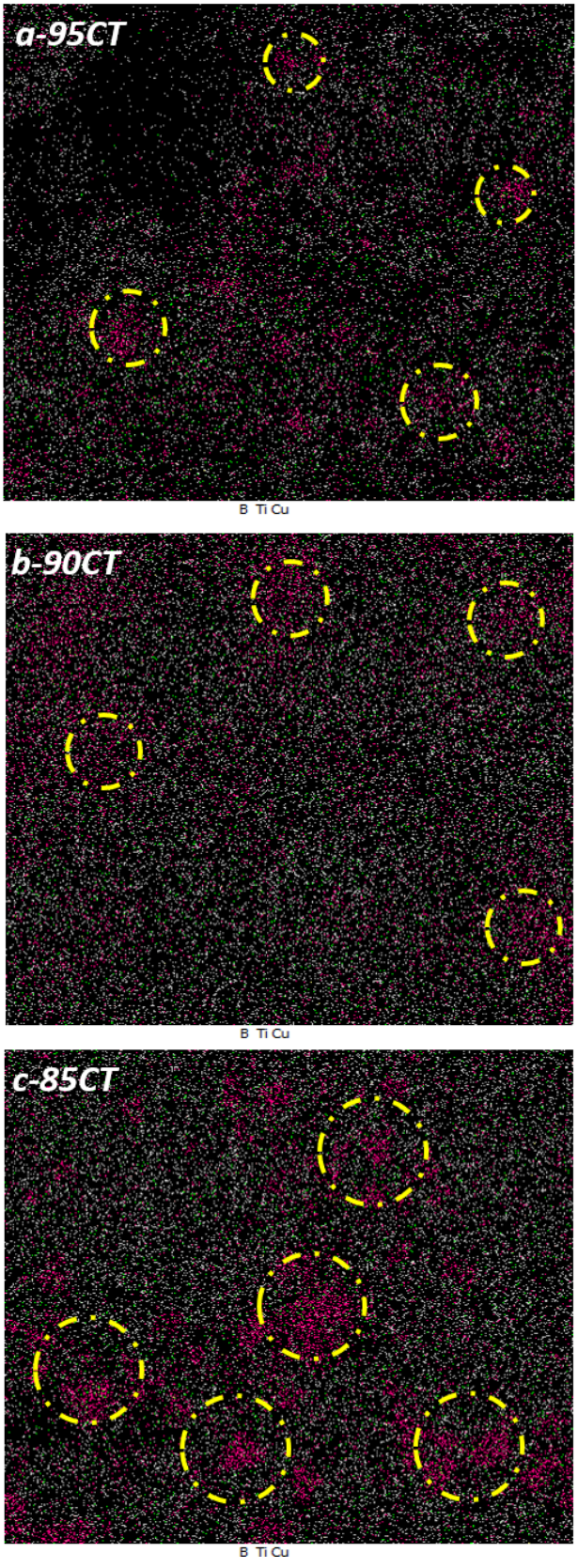

Fig. 2. MAP analysis of the achieved samples and presence of TiB_2 nanoparticles.

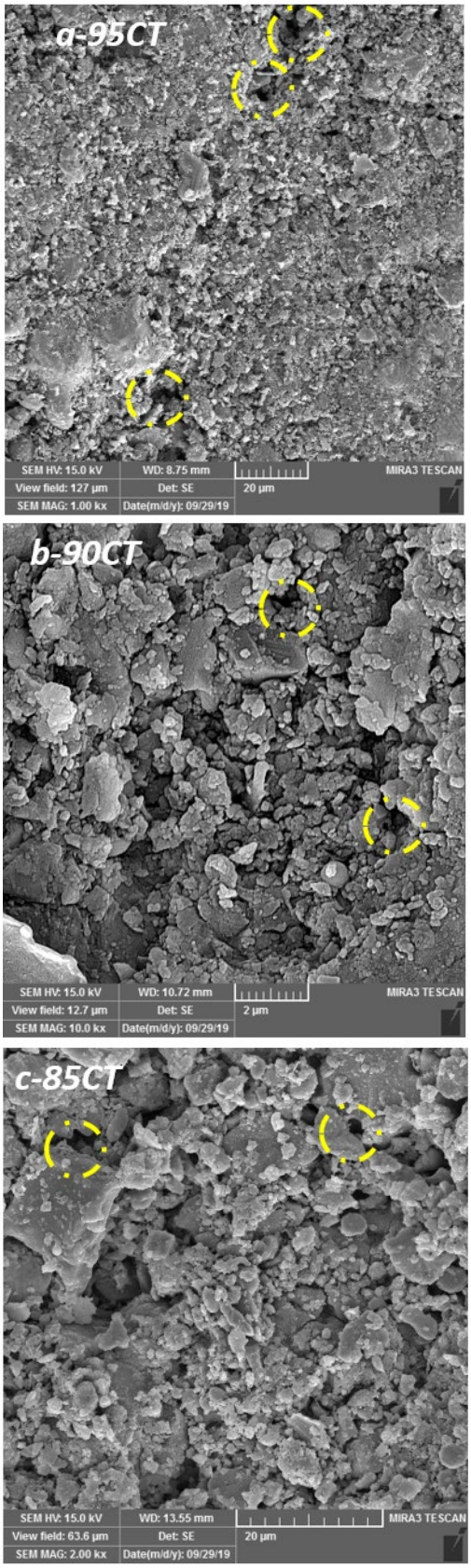

Fig. 3. FE-SEM images of morphology of the synthesized samples.

Table 2. Electrochemical parameters obtained from polarization curves.

Samples	Log I (A/cm^2)	E_{corr} (V)
95CT	-3.149	-0.275
90CT	-2.680	-0.182
85CT	-3.057	-0.169

than TiB_2 nanoparticles. Also, this indicates that the formation of solid solutions has a more significant effect on the microhardness values [25].

The morphology of the achieved nanocomposites was studied by field mission scanning electron microscopy (FE-SEM) and images are presented in Fig. 3. The dispersion of TiB_2 nanoparticles in the copper matrix is obvious. It is shown the smooth surface was obtained in all samples and the smoothest surface was obtained in sample 95CT where the minimum amount of reinforcement was added to the copper matrix. What is more, it is apparent that the formation of the voids and porosities has occurred within the sintering process of the samples at 900 °C, which are shown by circles in Fig. 3. For studying the surface topography and surface roughness variation, atomic force microscopy (AFM) analysis was carried out. The 3D plot of the surface morphologies is presented in Fig. 4. It is shown that the topography of the surface of the synthesized samples was changed by increasing the amount of the added reinforcements, and it was changed from round peaks topography to the smooth little sharp peaks.

The polarization curves of the synthesized samples are presented in Fig. 5. To calculate the corrosion parameters, the Stern-Geary equation was used which is presented in Eq. 1, where the R_P is the corrosion resistance and i_{corr} is the corrosion density, and calculated results are provided in Table 2. By comparing the results obtained from the curves, it is apparent that sample 95CT has the lowest i_{corr}, which equals -3.149 A/cm^2 and the highest corrosion resistance, which equals -0.275 V in comparison with others, which might be due to the presence of the lower amount of the reinforcement TiB_2 nanoparticles in this samples. In other words, by increasing the amount of TiB_2 nanoparticles, the polarization curves are shifted to the right side, to the lower value of corrosion potential and higher amount of corrosion density. These nanoparticles lead to some discontinuities on the surface of the sample and the local galvanic couple is activated within the corrosion mechanism.

Table 3. EIS results of samples.

Samples	R_1	R_2	CPE-T	CPE-P
95CT	7.456	14.6	0.0086	0.33
90CT	8.053	7.193	0.0098	0.73
85CT	13.1	15.13	0.0091	0.54

$$i_{corr} = \frac{b_a \times b_c}{2.303 \times R_p \times (b_a + b_c)} \quad (1)$$

where the b_a and b_c are the Tafel slopes of an anodic and cathodic branch of polarization curve respectively. R_p is the corrosion resistance and i_{corr} is the corrosion current density in A/cm^2. Also, 2.303 is the conversion coefficient of Ln to log.

To get further information on the electrochemical behavior of synthesized samples, electrochemical Impedance Spectroscopy (EIS) was performed in the 3.5 wt% solutions at room temperature. The fitted Nyquist curves are presented in Fig. 5 which illustrates a complete semicircle curve. Also, the equivalent circuit which is used to fit data is demonstrated in Fig. 6, and the electrical parameters corresponded to the corrosion parameters are presented In Table 3. The circuit consists of a solution resistance (R_1), and R_2 refers to corrosion resistance. Constant phase element (CPE) is related to the porosities capacitors and is a constant phase element characterizing the electrical properties of the porosities. All Nyquist curves show a capacitive loop (one time constant) which is related to the charge transfer at the interface and surface porosities. It is well-known that a higher diameter indicates a higher corrosion resistance. It is shown that sample 85CT has higher corrosion resistance. The calculated values for CPE-P indicate that porosities are acting like infinitive porosity and drop in IR [13]. It could be declared that the corrosion resistance can be attributed to the surface parameters achieved by the AFM test and it has a direct relation to the measured surface roughness. The achieved surface roughness for

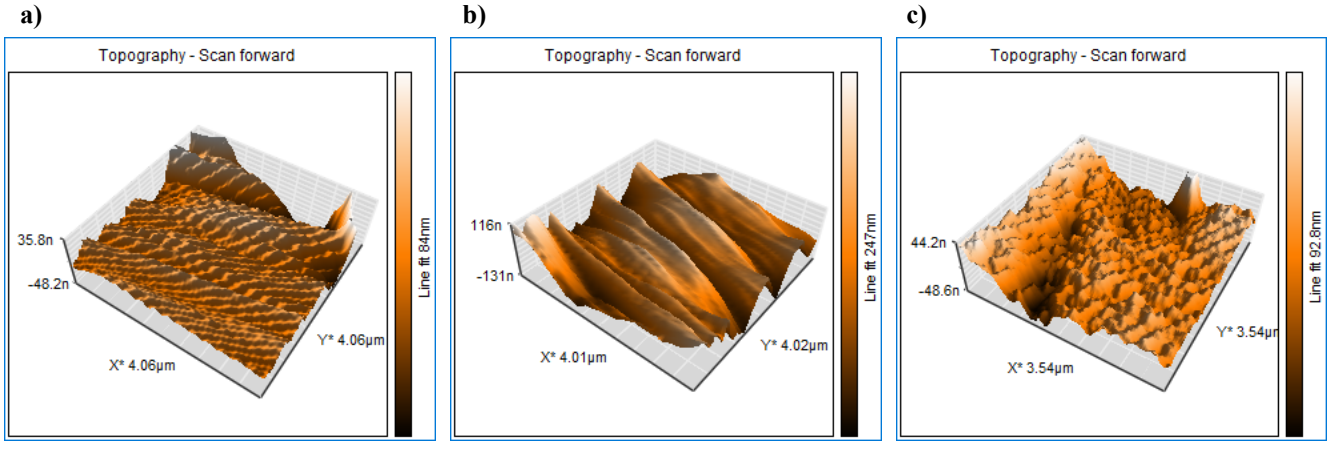

Fig. 4. AFM 3D plots of surface topography of a) 95CT, b) 90CT, and c) 85CT

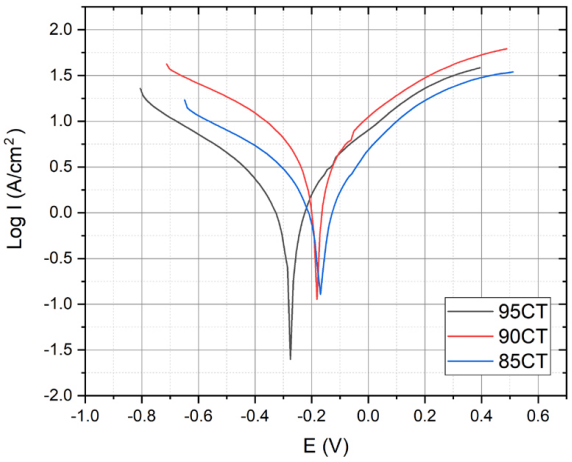

Fig. 5. Electrochemical polarization curves of samples.

samples 95CT, 90CT, and 85CT equals 15.06, 16.26, and 7.69 nm respectively. These outcomes could reveal that the surface morphology conditions including the surface roughness and the number of porosities have a more considerable effect than the formation of galvanic coupling on the corrosion behavior.

4. Conclusions

By adding TiB_2 nanoparticles the copper matrix nanocomposite was synthesized by in-situ method and sintering at 900 °C within 4 hours. The maximum surface microhardness was obtained at the sample with 15 wt% of reinforcement. Although more galvanic couples were formed in the sample with 15 wt% of TiB_2 nanoparticles, the effect of the surface roughness and the amount of the porosities are higher than these galvanic couples. Therefore, the best corrosion resistance was achieved in the sample with the maximum amount of reinforcement and it has a direct relation to the measured surface roughness. The surface morphology condition, including surface roughness and amounts of porosities, has a more significant effect on the corrosion behavior than the formation of galvanic coupling.

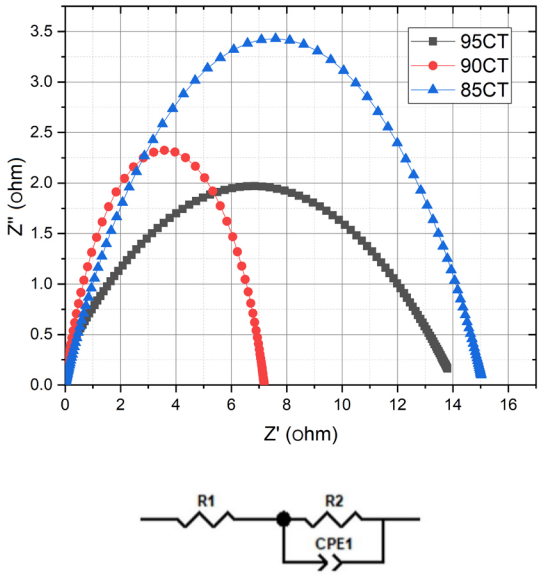

Fig. 6. Nyquist fitted curves of the samples.

CRediT authorship contribution statement

Hossein Aghajani: Supervision, Conceptualization, Writing-Original Draft.
Seyed Ali Naziri Mehrabani: Formal Analyis, Investigation, Methodology, Writing-Original Draft.
Arvin Taghizadeh Tabrizi: Conceptualization**,** Formal Analyis, Writing – review & editing.
Falih Hussein Saddam: Formal Analysis, Investigation.

Data availability

The data underlying this article will be shared on reasonable request to the corresponding author.

Declaration of competing interest

The authors declare no competing interests.

Funding and acknowledgment

The authors express their gratitude to the University of Tabriz for their generous financial support and for providing the necessary instruments and equipment essential for the successful completion of this study.

References

[1] F. Akhtar, S.J. Askari, K. Ali Shah, X. Du, S. Guo, Microstructure, mechanical properties, electrical conductivity and wear behavior of high-volume TiC reinforced Cu-matrix composites, Mater. Charact. 60 (2009) 327–336. https://doi.org/10.1016/j.matchar.2008.09.014.
[2] J.B Correia, H.A. Davies, C.M. Sellars, Strengthening in rapidly solidified age hardened Cu-Cr and Cu-Cr-Zr alloys, Acta Mater. 45 (1997) 177–190. https://doi.org/10.1016/S1359-6454(96)00142-5.
[3] S.C. Tjong, K.C. Lau, Properties and abrasive wear of TiB2/Al-4%Cu composites produced by hot isostatic pressing, Compos. Sci. Technol. 59 (1999) 2005–2013. https://doi.org/10.1016/S0266-3538(99)00056-1.
[4] J. Xu, W. Liu, Wear characteristic of in situ synthetic TiB2 particulate-reinforced Al matrix composite formed by laser cladding, Wear. 260 (2006) 486–492. https://doi.org/10.1016/j.wear.2005.03.032.
[5] Z.M. Du, J.P. Li, Study of the preparation of Al2O3sf.SiCp/Al composites and their wear-resisting properties, J. Mater. Process. Technol. 151 (2004) 298–301. https://doi.org/10.1016/j.jmatprotec.2004.04.077.
[6] F. Shehata, A. Fathy, M. Abdelhameed, S.F. Moustafa, Preparation and properties of Al2O3 nanoparticle reinforced copper matrix composites by in situ processing, Mater. Des. 30 (2009) 2756–2762. https://doi.org/10.1016/j.matdes.2008.10.005.
[7] F. Chi, M. Schmerling, Z. Eliezer, H.L. Marcus, M.E. Fine, Preparation of Cu-TiN alloy by external nitridation in combination with mechanical alloying, Mater. Sci. Eng. A. 190 (1995) 181–186. https://doi.org/10.1016/0921-5093(95)09617-5.
[8] P.K. Deshpande, R.Y. Lin, Wear resistance of WC particle reinforced copper matrix composites and the effect of porosity,

Mater. Sci. Eng. A. 418 (2006) 137–145. https://doi.org/10.1016/j.msea.2005.11.036.
[9] İ. Çelikyürek, N.Ö. Körpe, T. Ölçer, R. Gürler, Microstructure, properties and wear behaviors of (Ni3Al)p reinforced Cu matrix composites, J. Mater. Sci. Technol. 27 (2011) 937–943. https://doi.org/10.1016/S1005-0302(11)60167-9.
[10] S.C. Tjong, K.C. Lau, Tribological behaviour of SiC particle-reinforced copper matrix composites, Mater. Lett. 43 (2000) 274–280. https://doi.org/10.1016/S0167-577X(99)00273-6.
[11] G. Naseri Azari, A. Taghizadeh Tabrizi, H. Aghajani, Investigation on corrosion behavior of Cu–TiO2 nanocomposite synthesized by the use of SHS method, J. Mater. Res. Technol. 8 (2019) 2216–2222. https://doi.org/10.1016/j.jmrt.2019.01.025.
[12] J.P. Tu, N.Y. Wang, Y.Z. Yang, W.X. Qi, F. Liu, et al., Preparation and properties of TiB2 nanoparticle reinforced copper matrix composites by in situ processing, Mater. Lett. 52 (2002) 448–452. https://doi.org/10.1016/S0167-577X(01)00442-6.
[13] J.M. Torralba, F. Velasco, C.E. Costa, I. Vergara, D. Cáceres, Mechanical behaviour of the interphase between matrix and reinforcement of Al 2014 matrix composites reinforced with (Ni3Al)p, Compos. A: Appl. Sci. Manuf. 33 (2002) 427–434. https://doi.org/10.1016/S1359-835X(01)00104-X.
[14] T. Han, J. Li, N. Zhao, C. Shi, E. Liu, et al., In-situ fabrication of nano-sized TiO2 reinforced Cu matrix composites with well-balanced mechanical properties and electrical conductivity, Powder Technol. 321 (2017) 66–73. https://doi.org/10.1016/j.powtec.2017.08.019.
[15] A. Fathy, O. Elkady, A. Abu-Oqail, Production and properties of Cu-ZrO2 nanocomposites, J. Compos. Mater. 52 (2018) 1519–1529. https://doi.org/10.1177/0021998317726148.
[16] E.M. Salleh, Z. Hussain, Characterization of tantalum carbide reinforced copper composite developed using mechanical alloying, Key Eng. Mater. 471–472 (2011) 798–803. https://doi.org/10.4028/www.scientific.net/KEM.471-472.798.
[17] S.S. Javaherian, H. Aghajani, P. Mehdizadeh, Cu-TiO2 composite as fabricated by SHS method, Int. J. Self-Propag. High-Temp. Synth. 23 (2014) 47–54. https://doi.org/10.3103/S1061386214010051.
[18] S.F. Moustafa, S.A. El-Badry, A.M. Sanad, B. Kieback, Friction and wear of copper-graphite composites made with Cu-coated and uncoated graphite powders, Wear. 253 (2002) 699–710. https://doi.org/10.1016/S0043-1648(02)00038-8.
[19] Y. Chen, X. Zhang, E. Liu, C. He, C. Shi, et al., Fabrication of in-situ grown graphene reinforced Cu matrix composites, Sci. Rep. 6 (2016) 19363. https://doi.org/10.1038/srep19363.
[20] C.L.P. Pavithra, B.V. Sarada, K.V. Rajulapati, T.N. Rao, G. Sundararajan, A new electrochemical approach for the synthesis of copper-graphene nanocomposite foils with high hardness, Sci. Rep. 4 (2014) 4049. https://doi.org/10.1038/srep04049.
[21] Y. Hu, O.A. Shenderova, Z. Hu, C.W. Padgett, D.W. Brenner, Carbon nanostructures for advanced composite, Rep. Prog. Phys. 69 (2006) 1847. https://doi.org/10.1088/0034-4885/69/6/R05.
[22] N. Sadeghi, H. Aghajani, M.R. Akbarpour, Microstructure and tribological properties of in-situ TiC-C/Cu nanocomposites synthesized using different carbon sources (graphite, carbon nanotube and graphene) in the Cu-Ti-C system, Ceram. Int. 44 (2018) 22059–22067. https://doi.org/10.1016/j.ceramint.2018.08.316.
[23] M.S. Motta, P.K. Jena, E.A. Brocchi, I.G. Solórzano, Characterization of Cu–Al2O3 nano-scale composites synthesized by in situ reduction, Mater. Sci. Eng. C. 15 (2001) 175–177. https://doi.org/10.1016/S0928-4931(01)00272-7.
[24] S.A.N. Mehrabani, A.T. Tabrizi, H. Aghajani, H. Pourbagheri, Corrosion Behavior of SHS-Produced Cu–Ti–B Composites, Int. J. Self-Propag. High-Temp. Synth. 29 (2020) 167–172. https://doi.org/10.3103/S1061386220030061.
[25] S.A. Javadi, S.N. Hokmabad, A.T. Tabrizi, H. Aghajani, Corrosion behavior, microstructure and phase formation of ternary Ni-Ti-Si nano composite synthesized by SHS method, Powder Metall. 64 (2021) 341–350. https://doi.org/10.1080/00325899.2021.1906564.